Understanding the Physics of Electrodynamic Shaker Performance

George Fox Lang and **Dave Snyder**, Data Physics Corporation, San Jose, California

The performance envelope of an electrodynamic shaker system is strongly influenced by three modes of vibration and the voltage/current capacities of the power amplifier that drives it. Other limiting factors are the designed stroke (displacement) of the table, the moving mass and the total mass of the shaker, the thermal power limit (i^2R) of the coil and the stress safety factor of the armature. This article will discuss a basic electromechanical shaker model, how to determine Maximum Drive performance for sinusoidal testing, the merits of pneumatic load-leveling suspensions and the often overlooked side effects of shaker isolation. It will also examine system performance from a power perspective and present a simple means of estimating maximum system performance.

The structure of an electrodynamic shaker bears some resemblance to a common loudspeaker but is more robust. At the heart of the shaker is a coil of wire, suspended in a fixed radial magnetic field. When a current is passed through this coil, an axial force is produced in proportion to the current and this is transmitted to a table structure to which the test article may be affixed.

Figure 1 shows the magnetic circuit used to create the intense magnetic field required by the shaker. A permeable (ferrous) inner pole piece transmits flux from one end of an axially magnetized permanent magnet or electromagnet, say, the North face. A permeable "back structure" conducts flux from the opposite pole of the magnet to a permeable disk with a hole in its center surrounding the inner pole piece. This creates a radial flux field in the air gap between the round face of the North-polarized inner pole piece and the round hole in South-polarized outer pole piece. The air-gap between these pole pieces is minimized to reduce the reluctance of the magnetic circuit thus maximizing the intensity of the fixed magnetic field.

The force provided by the machine is proportional to the magnetic flux passing through the coil, to the current flowing through the coil and to the length of wire within the flux field. In general, shaker coils use heavier conductors than speakers so that they may accommodate heavier currents.

The coil, coil form and table structure combination is called the armature assembly. The test object is rigidly mounted to the armature assembly. Some shakers have interchangeable armatures, providing a small table for high-g testing of light objects and a large table for mounting heavy objects. In older designs, the coil is wound around the outer diameter of a stiff, thin-walled tube. Modern armature designs typically use epoxy bonding techniques to affix a rigid epoxy-stabilized coil to a light magnesium table structure.

The armature must be accurately centered in the narrow gap between the inner and outer poles. It must be allowed to move axially while being restrained from all other motions. This is accomplished by a soft elastic suspension system. In small shakers, a pierced compliant disk provides radially distributed cantilevers between the load table and the shaker body. In larger units, guide rollers support and center the armature while separate elastomeric shear elements provide the axial compliance.

This compliant connection between the armature assembly and the shaker body forms an obvious spring/mass/damper vibration system with one *degree-of-freedom*. Here, the test object and armature assembly move together, relative to the shaker body. Adding two more degrees-of-freedom completes the shaker mechanical model. Firstly, the armature structure is recognized as being elastic rather than rigid. This is modeled by treating the coil and table as separate masses connected

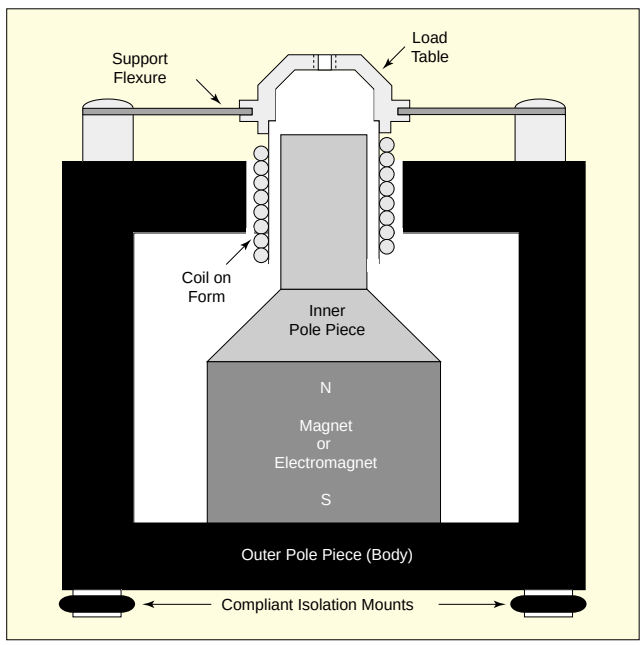

Figure 1. Soft iron pole pieces bend and concentrate almost all of the magnetic field into a very narrow gap. The armature coil is centered in this gap using support flexures (for small shakers) or rollers (for large shakers). Significant compliant connections include the support flexures, the isolation mounts and the connection between the coil and the Load Table

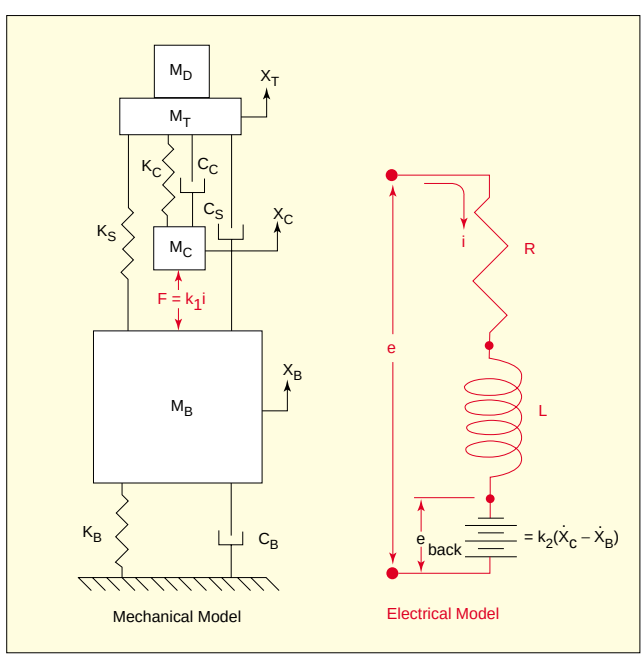

Figure 2. The mechanical and electrical parts of a shaker are cross-coupled. The mechanical system is excited by a force proportional to electrical current, while the electrical circuit is excited by an internal voltage (back-emf) proportional to mechanical velocity. The amplifier drives the electrical circuit providing an external voltage e and current i.

Figure 3. Data Physics model S-100 shaker.

by a spring and damper. Secondly, shakers are frequently isolated from the building floor by use of compliant mounts that allow the entire machine to translate vertically. This is modeled by attaching the shaker body mass to ground using a spring and damper.

The shaker's electrical model must account for the resistance and inductance of the armature coil. The coil resistance R defines the **minimum** impedance exhibited at the shaker input terminals. This resistance increases substantially with temperature (the resistance of copper wire increases by about 40% per 100° C) and increases slightly with frequency (due to the skin effect). The coil inductance L is large because the coil couples strongly with the iron of the pole pieces, causing the complex electrical impedance, equal to $R + j\omega L$, to increase with frequency.

The interplay between the electrical and mechanical domains is not a "one-way street." When the coil moves within the magnetic field, a voltage is generated across the coil in proportion to the velocity. This "back EMF" is seen in the electrical domain as an increase of the coil impedance and reflects the mechanical activity into the electrical circuit. These interactions are reflected in the composite mechanical-electrical model of Figure 2.

The equations for this system may be stated:

$$\begin{bmatrix} M_C & 0 & 0 & 0 \\ 0 & M_T + M_D & 0 & 0 \\ 0 & 0 & M_B & 0 \\ 0 & 0 & 0 & 0 \end{bmatrix} \begin{Bmatrix} \ddot{X}_C \\ \ddot{X}_T \\ \ddot{X}_B \\ 0 \end{Bmatrix} + \begin{bmatrix} C_C & -C_C & 0 & 0 \\ -C_C & C_C + C_S & -C_S & 0 \\ 0 & -C_S & C_B + C_S & 0 \\ k_2 & 0 & -k_2 & L \end{bmatrix} \times$$

$$\begin{Bmatrix} \dot{X}_C \\ \dot{X}_T \\ \dot{X}_B \\ di/dt \end{Bmatrix} + \begin{bmatrix} K_C & -K_C & 0 & -k_1 \\ -K_C & K_S + K_C & -K_S & 0 \\ 0 & -K_S & K_B + K_S & k_1 \\ 0 & 0 & 0 & R \end{bmatrix} \begin{Bmatrix} X_C \\ X_T \\ X_B \\ i \end{Bmatrix} = \begin{Bmatrix} 0 \\ 0 \\ 0 \\ e \end{Bmatrix}$$

The frequency domain solution to these system equations is a set of four transfer functions relating the mass motions and driving voltage to the applied current. These are shown in Figure 4.

Three modes of vibration dominate the mechanical response. At very low frequency (often below the range of operation), the compliant isolation mounts allow the entire shaker to translate as a rigid body with almost no relative motion between the components. This deformation shape is termed the Isolation Mode. In the low end of the operating range (10 to 40 Hz, typical) the Suspension Mode dominates. In this shape, the table and coil move together relative to the shaker body. Motion in this mode is limited by the design stroke of the machine. At or beyond the high frequency limit of operation, the (undesired) Coil Mode is encountered. Here, the coil moves out-of-phase

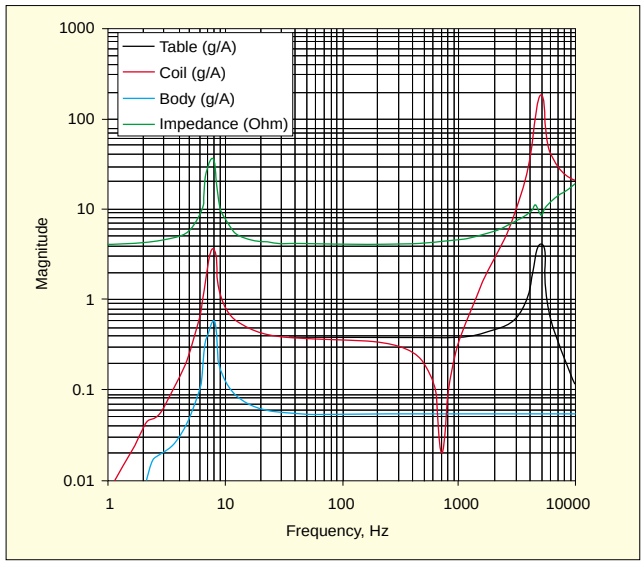

Figure 4. The four solution transfer functions relating the drive voltage (top curve) and motions of coil (middle curve – with pronounced antiresonance), table and body (bottom curve) to applied current as functions of frequency.

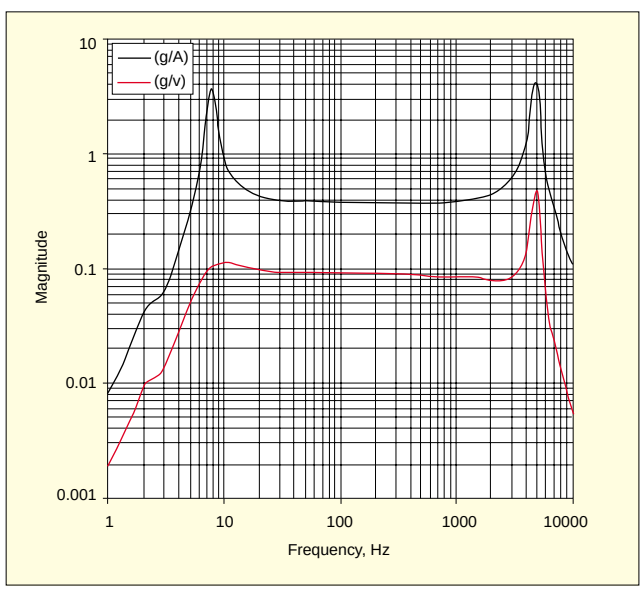

Figure 5. Transfer functions describing table acceleration per amp (upper curve) and per volt (lower curve) show the damping induced by the 'back-emf.'

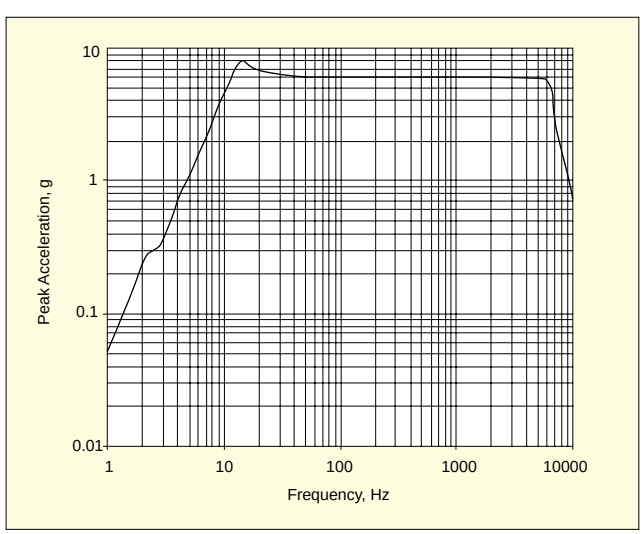

Figure 6. Maximum table acceleration versus frequency while driving 10 kg test object and respecting all shaker system limits.

Simplified Shaker Performance Envelope

A conservative estimate of a shaker's maximum performance envelope can be drawn from nine spec-sheet numbers. When a log-log axis plot is used as shown in Figure A, only eight points need to be defined and connected by straight-line segments. This provides a graphic view of the acceleration potential over the entire range of payloads.

From the system specifications, determine:

f_{min} = minimum operating frequency (Hz)
f_{max} = maximum operating frequency (Hz)
F_{rate} = sinusoidal force rating (N pk)
S_{rate} = stroke rating of shaker (mm pk-pk)
M_{mov} = moving mass (kg)
M_{total} = total mass of shaker and trunnion (kg)
M_{rate} = rated maximum test object mass (kg)
K_s = stiffness of shaker suspension (N/m)
V_{rate} = maximum bare table velocity (m/s pk)

Compute the derated stroke used in the blue "With Device Under Test" trace.

δ_{static} = static deflection of suspension (mm)
= 9800 M_{rate}/K_s for a passive suspension
= 0 with load leveling
IDF = isolation derating factor (ratio)
= 1 for hard-mounted shaker
= $(M_{total} - M_{mov})/(M_{total} + M_{rate})$ when the shaker is isolated. Note: when hard-mounted to an isolated slab, add slab mass to M_{total}
S_{derate} = derated stroke for full payload (mm)
= $IDF(S_{rate} - 2\delta_{static})$

Calculate VB, the peak velocity at point B: $VB = K_s S_{rate}/2000M_{mov}$ (m/s pk). If VB exceeds V_{rate}, plot the (black) bare-table envelope by connecting points A, B and C. Otherwise, plot A to D to E to C.

f_A = frequency at point A (Hz) = f_{min}
g_A = acceleration at point A (g pk) = $2(\pi F_{min})^2 S_{rate}/9800$
f_B = frequency of point B (Hz) = $\sqrt{K_S / M_{mov}}/2\pi$
g_B = acceleration at point B (g pk) = $F_{rate}/(9.8M_{mov})$
f_C = frequency at point C (Hz) = f_{max}
g_C = acceleration at point C (g pk) = $F_{rate}/(9.8M_{mov})$
f_D = frequency of point D (Hz) = $1000V_{rate}/(\pi S_{rate})$

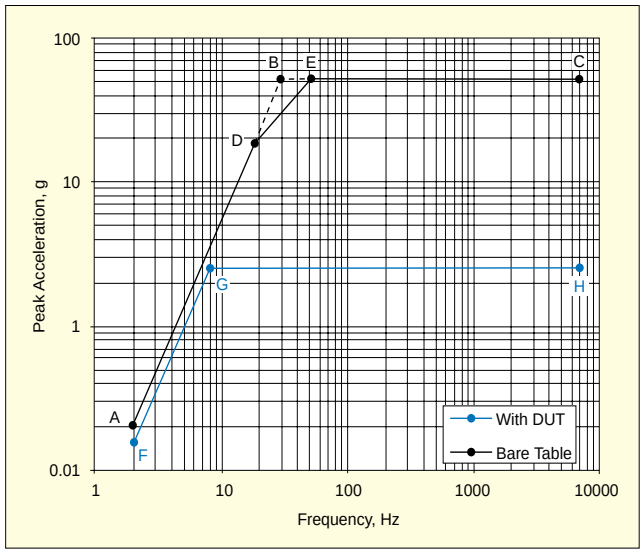

Figure A. Identification of envelope plotting points.

g_D = acceleration at point D (g pk) = $2(\pi F_D)^2 S_{rate}/9800$
f_E = frequency at point E (Hz) = $F_{rate}/(2\pi M_{mov} V_{rate})$
g_E = acceleration at point E (g pk) = $F_{rate}/(9.8M_{mov})$
f_F = frequency at point F (Hz) = f_{min}
g_F = acceleration at point F (g pk) = $2(\pi F_{min})^2 S_{derate}/9800$
f_G = frequency of point G (Hz) = $\sqrt{K_S/(M_{mov} + M_{rate})}/2\pi$
g_G = acceleration at point G (g pk) = $F_{rate}/[9.8(M_{mov} + M_{rate})]$
f_H = frequency at point H (Hz) = f_{max}
g_H = acceleration at point H (g pk) = $F_{rate}/[9.8(M_{mov} + M_{rate})]$

Constructing this "back of an envelope" overview of a shaker system's performance provides a surprisingly comprehensive understanding of the equipment's capability. Comparing this simple envelope with the corresponding detailed model (for our 650 N shaker in trunnion-isolated configuration) shows that the simple calculations are conservative as shown in Figure B. That is, your shaker will be able to provide the g-versus-frequency drive capability of your simple plot (and can actually

with the table as the elastic table/armature structure is deformed. Excessive excitation of this mode can damage the vibrator.

For purposes of example, the characteristics of the medium-size electromagnetic shaker shown in Figure 3 will be used. This machine is capable of delivering 650 N (145 lb) peak sine force to a test object weighing as much as 25 kg (55 lb) over a frequency range of 2 to 7000 Hz. It has a 25.4 mm (1 in) peak-to-peak stroke capability, a 1.5 m/s (59 in/s) peak velocity rating, a suspension stiffness of 22 kN/m (126 lb/in), a moving mass of 1.3 kg (2.86 lb), and an 8 ohm coil with an 11.2 (RMS) Ampere rating. The shaker and trunnion weigh 80 kg (176 lb). This shaker is equipped with base isolators and an automatic pneumatic load-leveling system.

The companion power amplifier delivers up to 11.2 A (RMS) current with a drive voltage of up to 90 V (RMS). The following figures assume a (dynamically inert) test item weighing 10 kg (22 lb) attached to the 80 mm (3.15 in) diameter drive table.

When the system is described by current-driven transfer functions, as shown in Figure 4, the effect of electromagnetic damping is not evidenced. These plots reflect only the structural damping terms, those that could be measured with external excitation applied to the shaker *with its drive coil unterminated*. These same low damping factors are at play when the shaker is driven by a *transconductance* or 'current' amplifier.

In contrast, expressing the system motions as voltage-driven transfer functions reflects the very significant electromagnetic damping applied by the cross-coupling terms between the electrical and mechanical components of the system. This is clearly shown by Figure 5 which compares table motion per Amp and per Volt. When connected to an audio 'voltage' amplifier, these higher damping factors are present.

Determining Maximum Drive Performance

The solution transfer functions and known system operating limits allow the maximum available sinusoidal output of the shaker at any frequency to be determined. This is accomplished by determining the largest current (at each frequency) that does *not* exceed:

- the (thermally determined) maximum RMS coil current
- the maximum RMS current capacity of the amplifier
- the maximum RMS voltage capability of the amplifier
- the stroke capability ($X_T - X_B$) of the shaker
- the maximum armature force capability

This composite current, shown in Figure 7, is "played-through" the transfer functions of Figure 4 to derive the mass motions and drive voltage of the system when it provides maximum excitation to the specified test object. Under these same conditions, other variables including the floor reaction force may be deduced from the simulation. Since the mathematical model is driven by a small number of measurable parameters, examining variations in the operating configuration is straightforward.

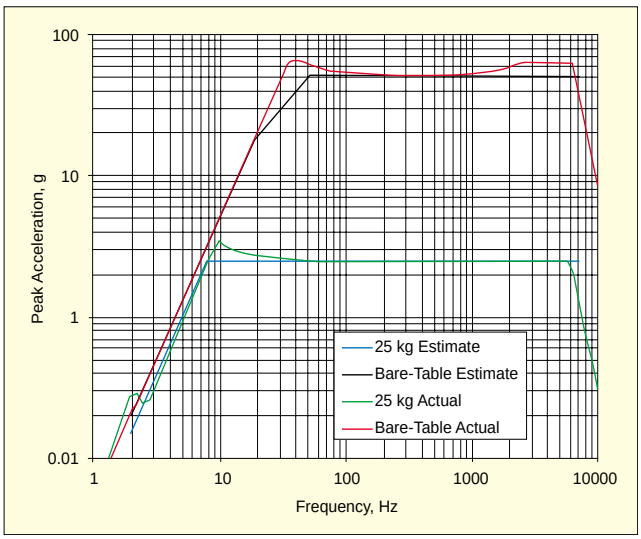

Figure B. Comparison of simple envelope with detailed simulation shows basic agreement. Shaker can actually exceed the "back of an envelope" expectations around the suspension resonance and at high frequency with a light payload.

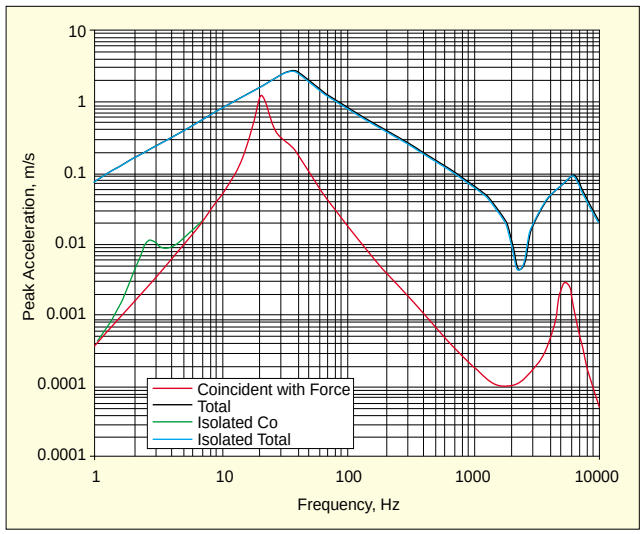

Figure C. Comparison of total coil velocity and force-coincident component of velocity during bare-table test. Data for both hard-mounted and trunnion-isolated shaker shown.

do a little better).

The detailed model discloses a higher performance level near the suspension resonance than does the simple envelope. In particular, the "constant velocity" slope is exceeded. This deserves a little explanation.

The *bare-table velocity* limit, V_{rate}, is not a structural limitation; it is an *electrical* one. This specification reflects the power amplifier's maximum voltage output and the 'back-emf' generation capability of the shaker. V_{rate} is conventionally evaluated at an '$F = Ma$' level of sophistication in accordance with:

$$V_{\text{rate}} = 2\left[(e_r i_r) - i_r^2 R\right] / F_{\text{rate}}$$

. . . where e_r is the maximum RMS voltage that the power amplifier can provide, i_r is the maximum RMS current that the shaker coil can tolerate (with specified cooling) and F_{rate} is the *peak* force value the machine can deliver.

However, this equation is only an approximation. The derivation of this relationship ignores phase (never a good idea!) and the simple envelope plot assumes the result is valid over the frequency range f_D to f_E. In fact, the approximation is only reasonable at a single frequency (approximately equal to f_D) as illustrated by the velocity plot of Figure C.

At that single frequency where the force-coincident component of velocity (red) is essentially equal to the total velocity (black), the V_{rate} equation is a reasonable model. This unique frequency is that at which maximum system efficiency is realized (see Figure 16). The approximation does not hold over a broader frequency span and thus the simple estimate is very conservative in this region.

The envelope comparison also shows that more aggressive excitation is possible at high frequency with light load as the "back of an envelope" estimate does not consider secondary effects of the coil resonance. Within the top decade of frequency, bare-table operation is actually limited first by current, then by force and finally by voltage.

Isolation Considerations

Figure 8 presents the reaction forces applied to the laboratory floor by the shaker. In the upper trace, the shaker is hard-mounted directly to the floor which experiences force levels greater than those seen by the test object. In the center trace, the isolation air-mounts at the base of the shaker are used to reduce floor vibration by better than an order of magnitude. In the bottom trace, the shaker is hard-mounted to a 1000 kg slab that is isolated from the building at a frequency of 0.5 Hz with 1% damping. This provides another order of magnitude reduction in building forces.

Figure 9 presents the low frequency end of the maximum table acceleration plot for these three configurations. Note that the slab mounted response essentially overlays the rigid mounting case, while the air-mount isolated configuration shows a **loss of effective stroke** due to the isolation.

In general, a shaker's stroke must be 'derated' when the shaker is mounted on an isolation system. When the body of the shaker is allowed to 'float,' rather than being tied to ground, it is forced to move in phase opposition to the drive-table by a force equal and opposite that driving the table. This relative motion reduces the stroke available to accelerate the test object by a factor of $M_B/(M_B + M_D + M_T + M_C)$. When the shaker is hard-mounted to a large isolated slab, the slab mass becomes part of M_B causing the stroke-reduction factor to approach 1.

Clearly, the preferred installation is to hard-mount the shaker to a large slab isolated from the laboratory building at a low frequency. Unfortunately, this option is not always available and an isolation system at the trunnion base is a practical alternative. Care must be taken in the design of such a mounting, however.

In general, local isolation systems must be tuned to a higher frequency than slab systems. This is done to minimize rocking motions possible when the test payload CG is not aligned with the drive axis, because the center of gravity of the shaker and payload are well above the rotational elastic axis of the base-mounted isolators. In Figures 10 and 11, the air-mounts are configured to provide a tuned frequency of 2.5 Hz. These figures illustrate the critical influence of the isolation *damping factor*.

Figure 10 shows the maximum possible table acceleration while driving a 10 kg test object with focus on the stroke-limited low frequency end. Note that a relatively high damping factor (20% in this case) is required to preclude losing significant stroke capability at the anti-resonant 'notch' between the isolation and suspension mode resonances. At frequencies above the anti-resonance bandwidth, the isolated system provides $M_B/(M_B + M_D + M_T + M_C)$ of the unisolated stroke, regardless of the damping factor.

Figure 11 illustrates the effect of isolation damping on floor reaction forces. Note that all isolated systems present a transmissibility of 1 at 1.4 times the tuned frequency regardless of damping factor, in accordance with simple isolation theory. Below this frequency, the presence of isolation is a detriment

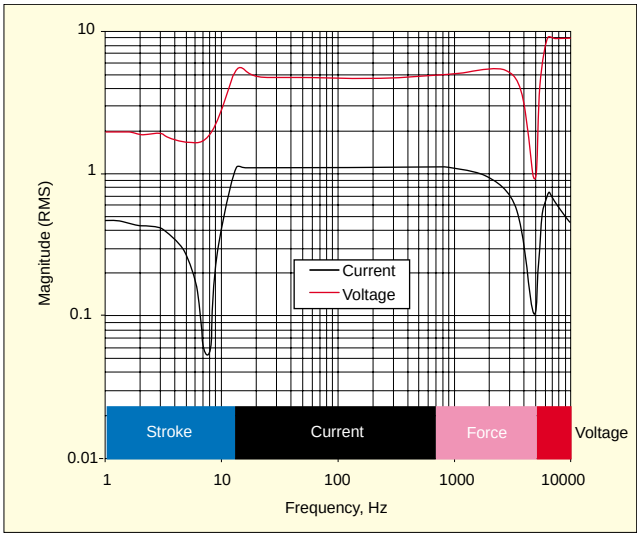

Figure 7. The voltage (upper curve) and current (lower curve) inputs required to achieve maximum table acceleration. Note that the acceleration-limiting factor changes from stroke to current to force to voltage with increasing frequency.

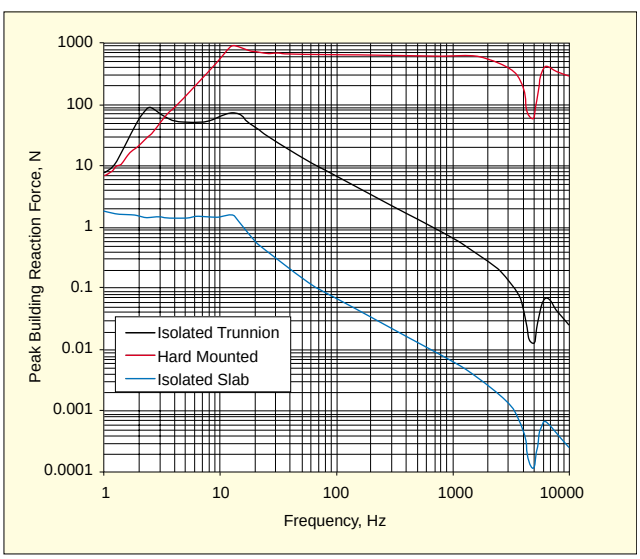

Figure 8. Floor reaction forces from three different shaker mounting configurations. The floor reaction forces are largest with rigid mounting (upper curve) and smallest with an isolated slab (lower curve). The commonly used isolation mounts (middle curve) reduce the reaction forces at most, but not all, frequencies.

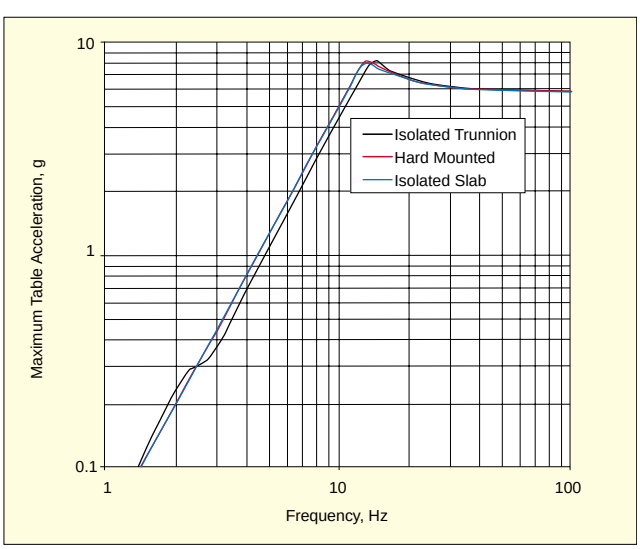

Figure 9. Maximum table acceleration in three mounting configurations shows effective stroke loss due to trunnion isolation.

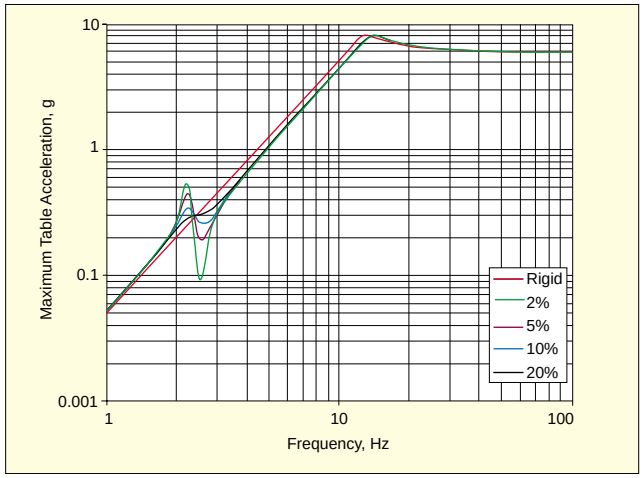

Figure 10. Effect of trunnion-base isolation damping factor on stroke loss.

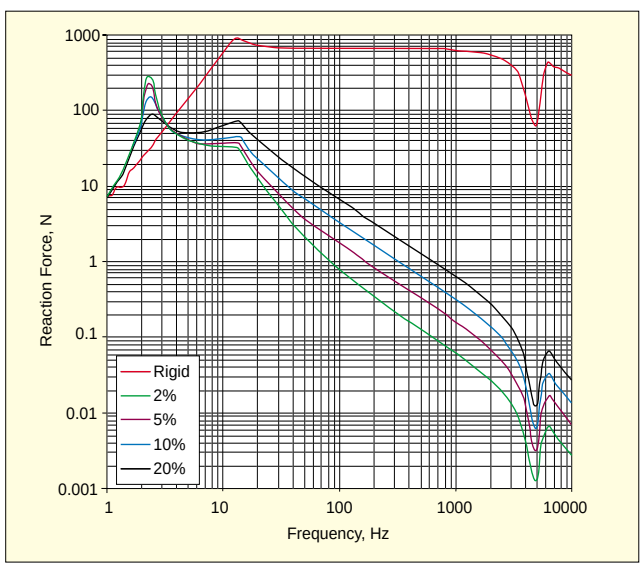

Figure 11. Effect of trunnion-base isolation damping factor on floor reaction load.

and high damping levels minimize the low frequency vibration transmitted. This benefit comes at the cost of greater floor transmission across most of the operating frequency range.

Don't Be Passive About The Suspension!

Many older shakers and most small (permanent magnet) shakers are built with a 'passive' suspension system. Newer designs intended for qualification tests of heavy objects incorporate an 'active' or load leveling suspension. This is generally accomplished by using pneumatic pressure to bear the static weight of the test object, leaving the suspension flexures to bear only the dynamic variation. This approach provides the full stroke capability of the shaker, regardless of the payload weight.

In Figure 12 our shaker is hard-mounted and its load leveling system is disabled, rendering the suspension passive. Maximum possible table acceleration with various payloads is presented. Figure 13 presents the same test set with load leveling enabled. The maximum acceleration levels differ in exactly the same ($F = Ma$!) manner in both plots. However, the load-leveled system maintains full stroke capability while the passive system surrenders it to payload as a "static deflection" numerically equal to $M_D g/K_S$. With load leveling, the static position of the table is always at the shaker's mid-stroke position.

It is possible to accomplish the same objective by other means, but none are as convenient as an automatic pneumatic sub-system. External suspensions can be created and tuned for a specific test, but such effort is not always straightforward or

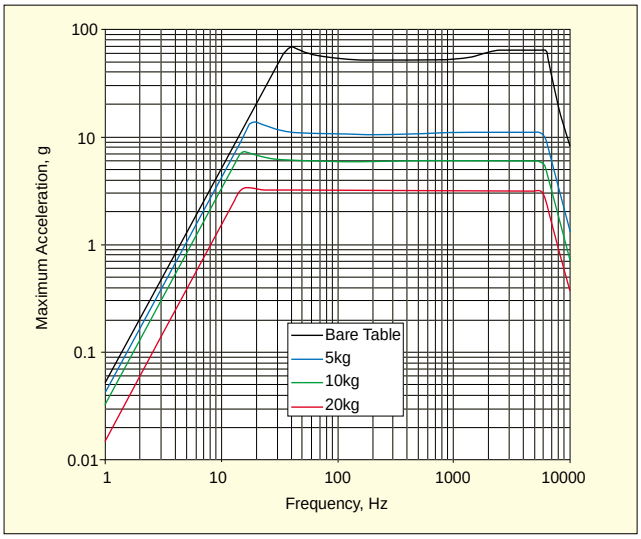

Figure 12. Effect of payload weight on maximum table acceleration without load leveling.

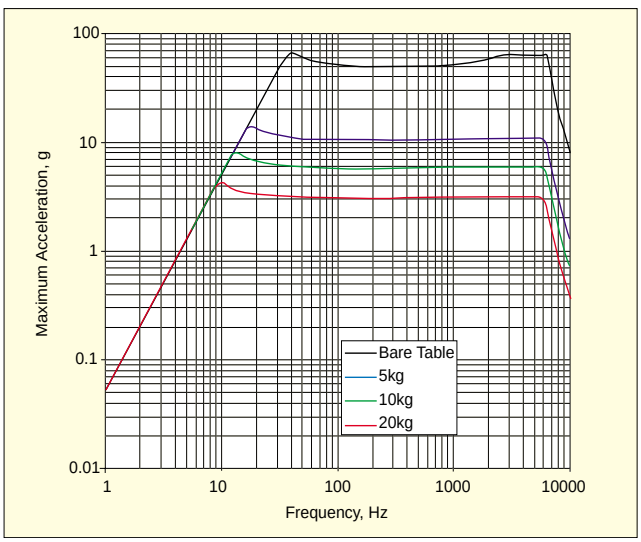

Figure 13. Effect of payload weight on maximum table acceleration with load leveling.

satisfactory. It is also possible to apply a DC voltage to the coil to 'raise' the static position of a loaded shaker back to mid-stroke. In most instances, this involves a system re-wire and the use of a DC power supply, further complicated if the power amplifier is *not* DC coupled. In any event, the effort is somewhat self-defeating as the DC current applied also heats the coil and thus the RMS current that may be used to shake must be reduced by the bias current. This reduces the available force rating of the machine.

Observations from a Power Perspective

Large shakers consume significant electrical power and convert it to heat. It is reasonable to be concerned with where those hard-earned kilowatt-hours are spent and where those unwelcome BTUs end up! The power amplifier applies a voltage to the shaker and supplies a current to it. A linear amplifier will do this with absolutely no more than 50 % efficiency while a digital amplifier can provide about 90 % efficient operation. Amplifier efficiency spells less heat in the lab space, normally a desirable thing. However, most of the power applied to the shaker will end up as heat, and this thermal load should be planned for.

AC electrical power is the product of RMS voltage and RMS current. However, this VA product contains two terms, the *active* or 'real' power (watts) that can actually do work and the *reactive* component (VAR) that cannot. You are billed for the

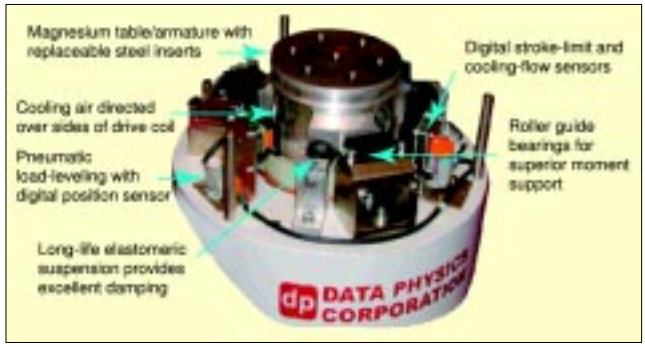

Figure 14. Anatomy of a modern shaker discloses space-age materials and system-level design.

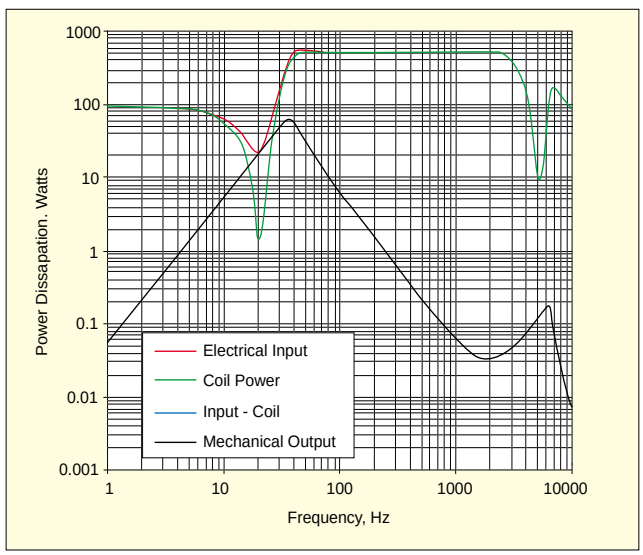

Figure 15. Reconciliaton of power within the shaker at maximum output (bare table operation in hard-mounted configuration). The electrical power input (upper curve) is converted into heat (middle curve) and mechanical power (bottom curve) which exactly overlays the difference between total input and coil heating.

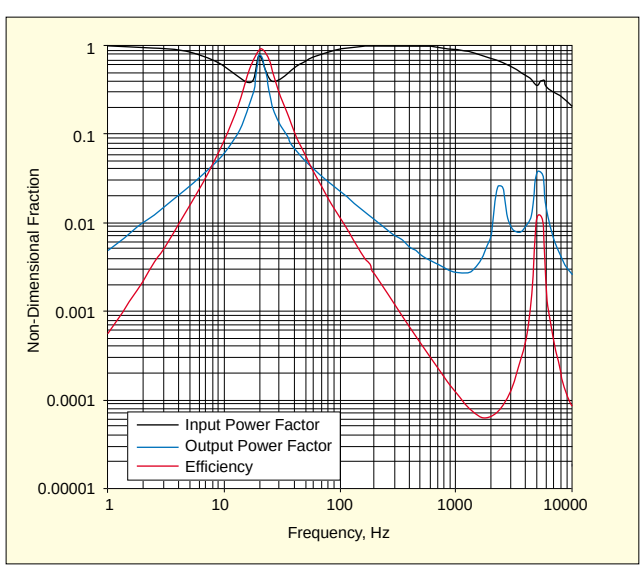

Figure 16. High Electrical Power Factor (top curve) indicates phase coincidence of voltage and current while low Mechanical Power Factor (middle curve) indicates quadrature phase between force and velocity. At most frequencies this results in less than 1% Efficiency (lower curve) for the conditions of Figure 15.

active watts consumed, where the voltage and current are *in phase*. Reactive power results from current in phase-quadrature with the voltage. The power transmission system must be sized for the vector resultant of these two orthogonal components. Hence power utilities provide lower rates to industrial

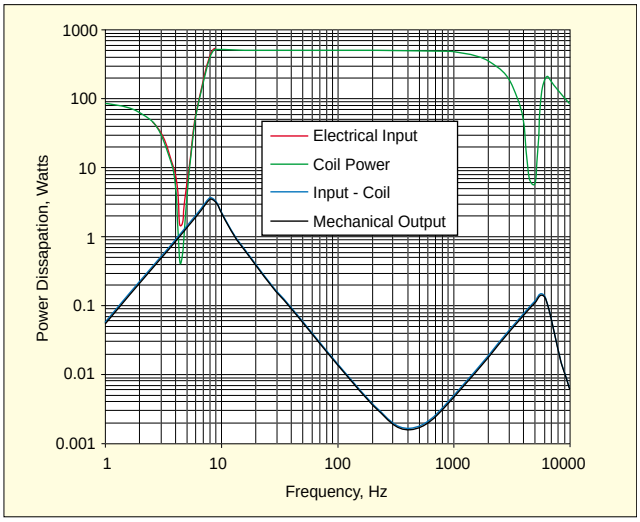

Figure 17. Distribution of power with 25 kg test object on shaker. Note general reduction in mechanical output power (lower curve) with essentially the same input requirement (upper curve), compared to Figure 15.

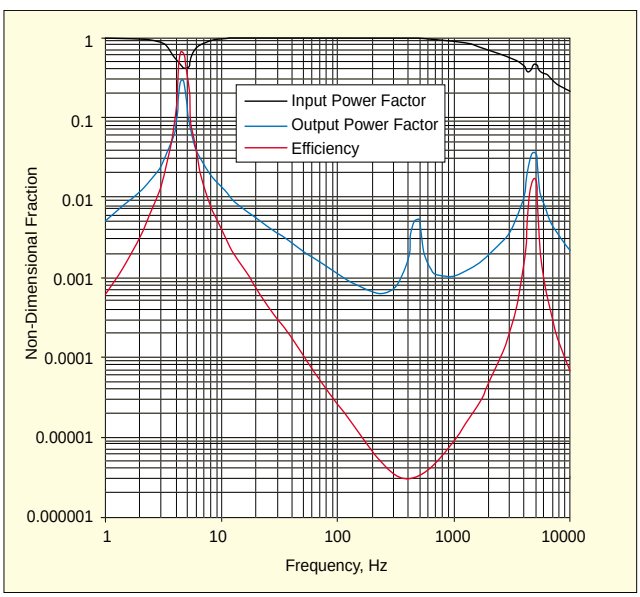

Figure 18. Fully laden shaker exhibits improved Input Power Factor and reduced Efficiency when compared to bare-table test of Figure 16. At most frequencies, much less than 0.1% of the electrical input is converted into mechanical power.

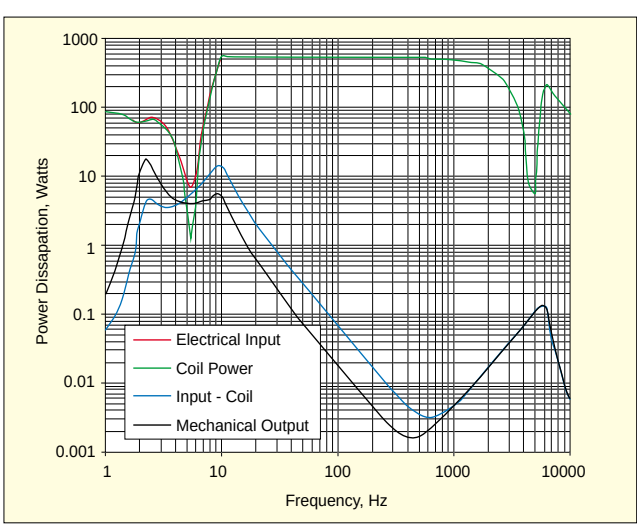

Figure 19. Repeat of 25 kg test on a shaker with trunnion base isolation (2.5 Hz, 20%). Note the mechanical output power no longer accounts for the full difference between input and coil dissipation.

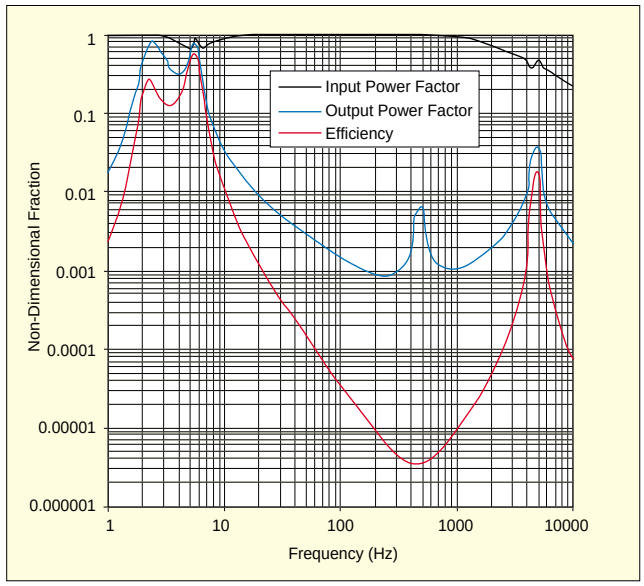

Figure 20. Efficiency and Power Factors exhibited during 25 kg shake on isolated shaker. In particular, note the improved efficiency (lowest curve) around the isolation-mode natural frequency caused by improved output power factor.

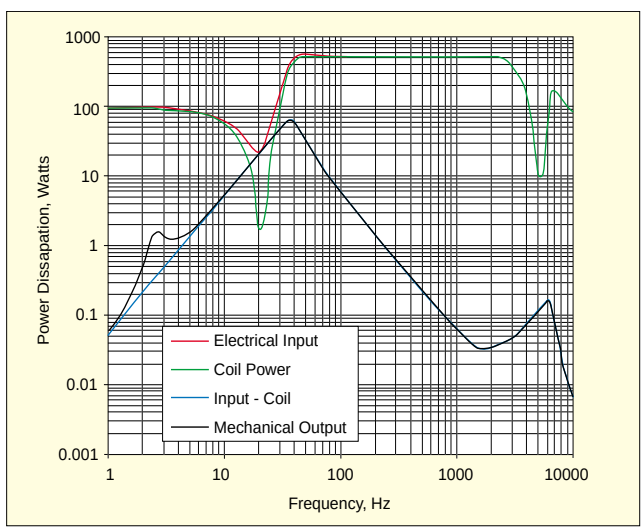

Figure 21. Power dissipations during a bare table test on the trunnion-isolated shaker. Note the 'unaccounted' added power near the isolation frequency.

customers who present a line-load with a high *power factor*, the cosine of the phase angle between voltage and current.

Mechanical power is directly analogous and may be expressed in the same units. The product of force and velocity is power. When these variables are sinusoidal, the RMS force times the RMS velocity times the cosine of the phase angle between force and velocity (the power factor) is the *active* mechanical power. This is the component that can do work. The quadrature *reactive* component merely shuttles retained system energy between potential and kinetic states.

Our shaker mathematical model contains all of the information necessary to evaluate the power dissipations within the system. In Figure 15 four different *active* power spectra are presented. The top line shows the total electrical power dissipated by the shaker operating with a bare table at maximum drive capability. The center trace shows the (i^2R) power dissipated as heat by the drive coil. The (completely obscured) line presents the difference between these two dissipations, the remaining electrical power available to drive the mechanical system. The black line presents the active *mechanical* power dissipated by the motion of the forced coil. This trace exactly matches the electrical power available to drive the mechanics.

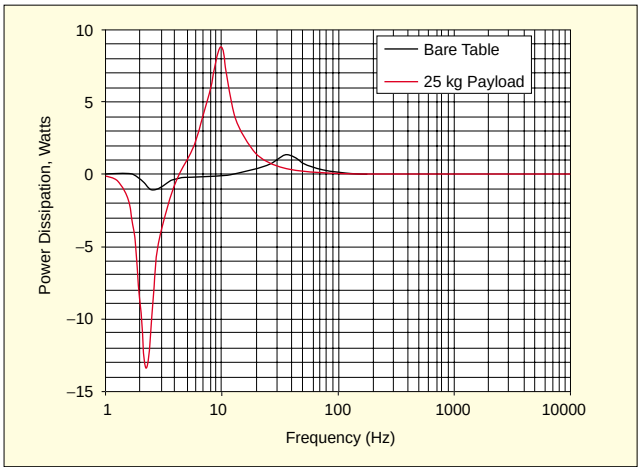

Figure 22. Active or 'real' power participation of the moving shaker body during isolated tests. Note the linear vertical axis necessary to show negative (powering) dissipation below the isolation resonance.

In Figure 16, three measures of power usage are presented. The black trace shows the *power factor* of the total electrical load while the blue trace presents the power factor of the mechanical output. The red *efficiency* trace expresses the active mechanical output power as a fraction of the active electrical input power. It is clear from these figures that the bulk of the electrical power entering the shaker leaves as heat due to dissipation in the voice coil. The low (less than 1.0) input power factor over much of the operating range indicates that the shaker is an inductive load at those frequencies.

The output power factor is low over most of the operating range, indicating the coil force and velocity are predominately in phase quadrature. The output power factor rises to nearly 1.0 in a narrow frequency range somewhat *below* the suspension resonance. It exhibits lesser peaks at the coil resonance and at the coil anti-resonance between the suspension and coil resonant frequencies.

Figures 17 and 18 present the same measurements as those of Figures 15 and 16, but the shaker now drives its maximum payload of 25 kg. The mechanical output power is greatly *reduced*, while the electrical input requirement remains relatively unchanged. That is, the efficiency decreases with payload.

As the load increases, the electrical input power factor improves over most of the operating range. That is, the system uses more of the VA potential available to it. The mechanical output power factor exhibits essentially the same signature described for the bare-table condition.

The preceding observations were made with the shaker hard-mounted to ground. Figures 19 and 20 repeat the 25 kg payload observations using a trunnion-isolated (2.5 Hz, 20%) shaker.

Comparing Figure 17 and 19 discloses an immediate difference due to isolation. The black *mechanical* output trace no longer overlays the blue difference between *electrical input* and *coil dissipation*. This difference is caused by motion of the 'floating' body reacting to the driving force reaction.

Comparing Figures 18 and 20 shows an astonishing difference: the efficiency actually *increases* in the low frequency 'neighborhood' of the isolation resonance! This is counter-intuitive; one would anticipate reduced efficiency across the operating range due to the need to 'power' the body's motion. This improved efficiency is explained, in part, by the improved output power factor in this region. The isolator functioned to phase-shift the coil velocity so that it was more nearly coincident with the coil force in this bandwidth.

Figure 21 repeats the bare-table test of Figure 15 using the isolated shaker. Again, *mechanical output* is discernable from the difference between *electrical input* and coil *dissipation*. It is clear in Figure 21 that the mechanical output *exceeds* the value of this electrical power difference.

Data Physics Shaker Offerings

Data Physics provides a broad range of electrodynamic shaker systems for use with SignalStar Vibration Controllers. Four design groups are offered: small permanent magnet shakers with force ratings of 2 to 100 lb, mid-range shakers (150 to 1800 lb), large systems (2400 to 8000 lb) and modal shakers (17 to 600 lb) optimized for 'stinger' drive.

Companion power amplifiers from 60 VA to 42 KVA are offered. All amplifiers are air-cooled and interlocked to integral protective shaker sensors for safe and simple operation.

Accessories include swivel trunnions, head expanders, stand-alone and mono-base slip tables, external load-support systems and L, T and Cube test fixtures. Data Physics can tailor a modern and precise system to match your single or multi-axis testing needs and power it with a pace-setting SignalStar Vector™ or Matrix™ controller.

Please visit www.dataphysics.com for more information on these products. The site also features a spread-sheet to evaluate your shaker system and a collection of related Application Notes.

Figure 22 provides the explanation. In this figure the *active* mechanical power dissipated by the shaker body velocity and the reaction force are plotted (for both the bare-table and 25 kg tests). Note that the vertical power axis of this figure is *linear* as the power has *negative* sign initially and crosses zero to become positive as frequency increases. That is, the isolation system acts first to *supply* added mechanical power to the output and at a higher frequency becomes a source of power dissipation. In a sense, the isolator functions as a mechanical power amplifier in the low frequency band.

Conclusions

A dynamic mathematical model involving three vibration modes (isolation, suspension and coil) with appropriate electromechanical cross coupling to a two element electrical circuit provides clear understanding of shaker system behavior. Maximum performance is understood by driving the model

with a composite current that respects stroke limit, drive coil power limitation, amplifier voltage/current limits and rated force capacity. A simple graphical means of conservatively estimating this behavior over the usable range of payload has been presented.

Current (as opposed to voltage) is clearly established as the desired reference for all structural transfer function relationships within a shaker. The ability to separate electromagnetic damping from other sources of damping has been demonstrated.

Low frequency performance is dictated by the shaker's design stroke and further limited by the need to isolate the machine from the laboratory building. The effects of isolation on achievable stroke have been investigated with particular emphasis on selecting appropriate damping factors. The interplay of maximum amplifier voltage in the neighborhood of suspension resonance has been reviewed with some interesting new findings regarding table velocity limit.

High frequency performance is shown to be limited by the "coil mode" resonance. Exceeding the rated high frequency limit can result in overstressing the armature structure of the machine. Clever design placement of the coil mode frequency and the resulting anti-resonance above suspension frequency can actually improve the high frequency performance of a shaker.

Power analysis discloses the electrodynamic shaker to be a thermodynamically inefficient machine. As machine payload is increased, efficiency decreases while line power factor improves. The laboratory thermal load (for fixed intensity shakes) is almost independent of test item weight. Power analysis discloses that an isolated system can be designed to improve mechanical delivery in the low frequency region. SV

To study the performance of conventional high strength electrodynamic shaker, this study has carried out a bare-table experiment on a V shaker of dual armature structure to measure its frequency response functions (FRF). The experiment system is shown in Fig. 2, including: Power amplifier, Hp-35670 dynamic signal analyzer, accelerometer and V shaker.Â Lang G. F. Understanding the physics of electrodynamic shaker performance. Sound and Vibration, Vol. 35, Issue 10, 2001, p. 24-33. [Search CrossRef]. Zhao C. S., Bao M. The research and the engineering application of electrodynamic vibrators. Journal of Nanjing University of Aeronautics & Astronautics, Vol. 25, Issue 5, 1993, p. 638-645, (in Chinese). [Search CrossRef]. Electrodynamic Shakerscdn2.hubspot.netA classical electrodynamic shaker test as considered in this article may be represented by the example de-picted in the Figure 1 (left). Figure 1: Real test loop (left) and Schematic test loop (right). The user introduces a target vibration prole (1) which will be used to produce a signal (2) sent to the shaker (4) through an amplier (3) to deliver the required power.Â [9] G. F. Lang, L. D. Snyder Understanding the Physics of Electrodynamic Shaker Performance, Journal of Sound and Vibration, Oct 2001. 1070. Proceedings of ISMA2016 including USD2016. pdfThe performance envelope of an electrodynamic shaker system is strongly influenced by three modes of vibration and the voltage/current capacities of the power amplifier that drives it. Other limiting factors are the designed stroke (displacement) of the table, the moving mass and the total mass of the shaker, the thermal power limit (i 2R) of the coil and the stress safety factor of the armature. This article will discuss a basic electromechanical shaker model, how to determine Maximum Drive performance for sinusoidal testing, the merits of pneumatic load-leveling suspensions and the often overlooked side effects of shaker isolation. It will also examine system performance from a power perspective and present a simple means of estimating maximum system performance. Understanding The Physics of Electrodynamic Shaker...scribd.com